Supporting Information

Growth of Fe_3O_4 Nanosheet arrays on Graphene by a Mussel-Inspired Polydopamine Adhesive for Remarkable Enhancement in Electromagnetic Absorptions

Fanbin Meng*, Wei Wei, Jingjing Chen, Xiangnan Chen, Xiaoling Xu, Man Jiang, Yong Wang, Jun Lu and Zuowan Zhou*

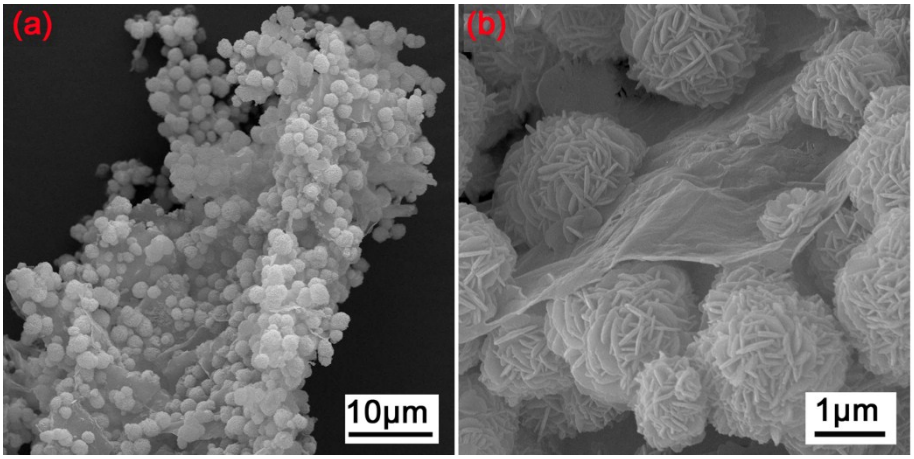

Fig. S1 SEM images of GO@iron alkoxide(a, b).

In order to investigate the growth mechanism of such architecture, each reaction stage was traced. When RGO@PDA mixed with $FeCl_3 \cdot 6H_2O$, The coated PDA can absorb and immobilize Fe^{3+} by the strong metal coordination ability of the catechol groups as proved by EDS[1,2] (Fig. S2a) and the subsequent reaction would be carried out on the surface of RGO@PDA. At the earch stage of EG-mediated process (treated 0 min), EG first coordinated with $FeCl_3$ to produce iron alkoxide, which precipitated to become the nuclei and quickly grew in the form of nanoparticles on the surfaces of the RGO@PDA, which served as "seed" (Fig. S2b). When treated 1 min, more particles were formed with larger size, which overlaied both surfaces of the RGO@PDA (Fig. S2c). With the reaction proceeded, primary particles undergo a structural modification to smooth their surfaces through traditional Ostwald ripening, and a specified nanosheet was formed via a secondary growth stage (Fig. S2d). It was in agreement with the previous report.[3] When treated 5 min, close and homogeneous iron alkoxide nanosheets grew on both surfaces of the RGO@PDA as shown in Fig. S2e. However, treated more than 10 min, the nanosheets on the RGO@PDA trended to aggregate into close-packed microspheres

composed of nanosheets shown in Fig. S2f.

[1] H. Lee, S. M. Dellatore, W. M. Miller, P. B. Messersmith, *Science*, 2007, **318**, 426.

[2] J. Ryu, S. H. Ku, H. Lee, C. B. Park, *Adv. Funct. Mater.*, 2010, **20**, 2132.

[3] L. S. Zhong, J. S. Hu, H. P. Liang, A. M. Cao, W. G. Song, L. J. Wan, *Adv. Mater.*, 2006, **18**, 2426.

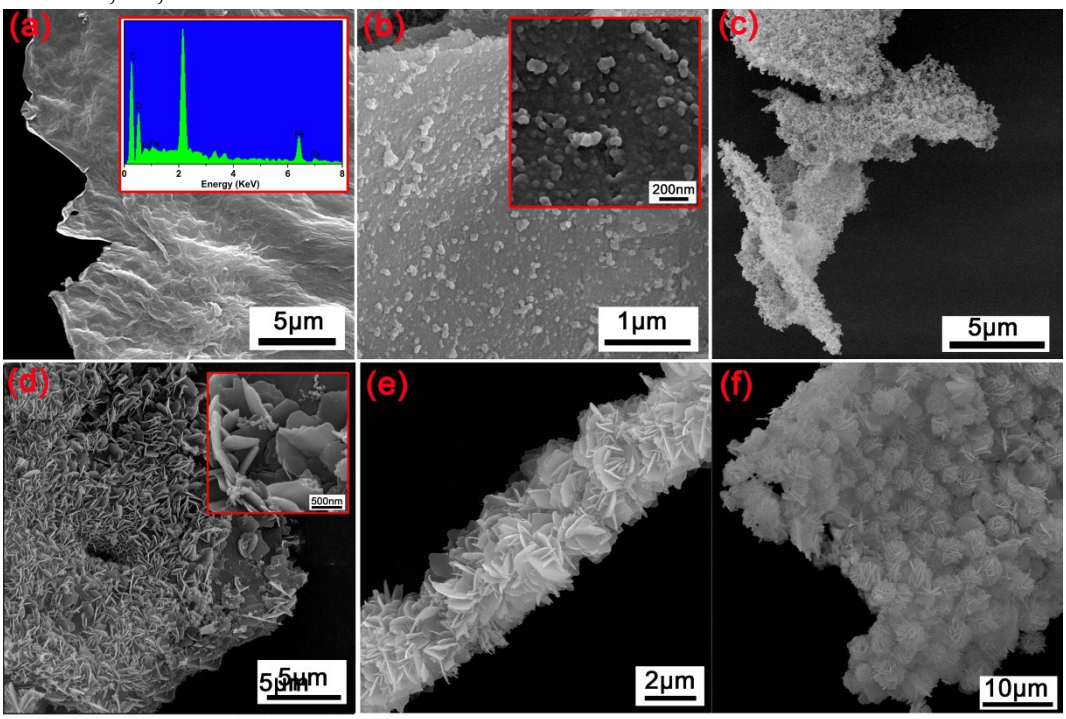

Fig. S2 SEM images of RGO@PDA (a), inset showing the corresponding EDS, and RGO@PDA@iron alkoxide collected at different intervals: (b) 0 min, (c) 1 min, (d) 3min, (e) 5 min, (f) 10 min.

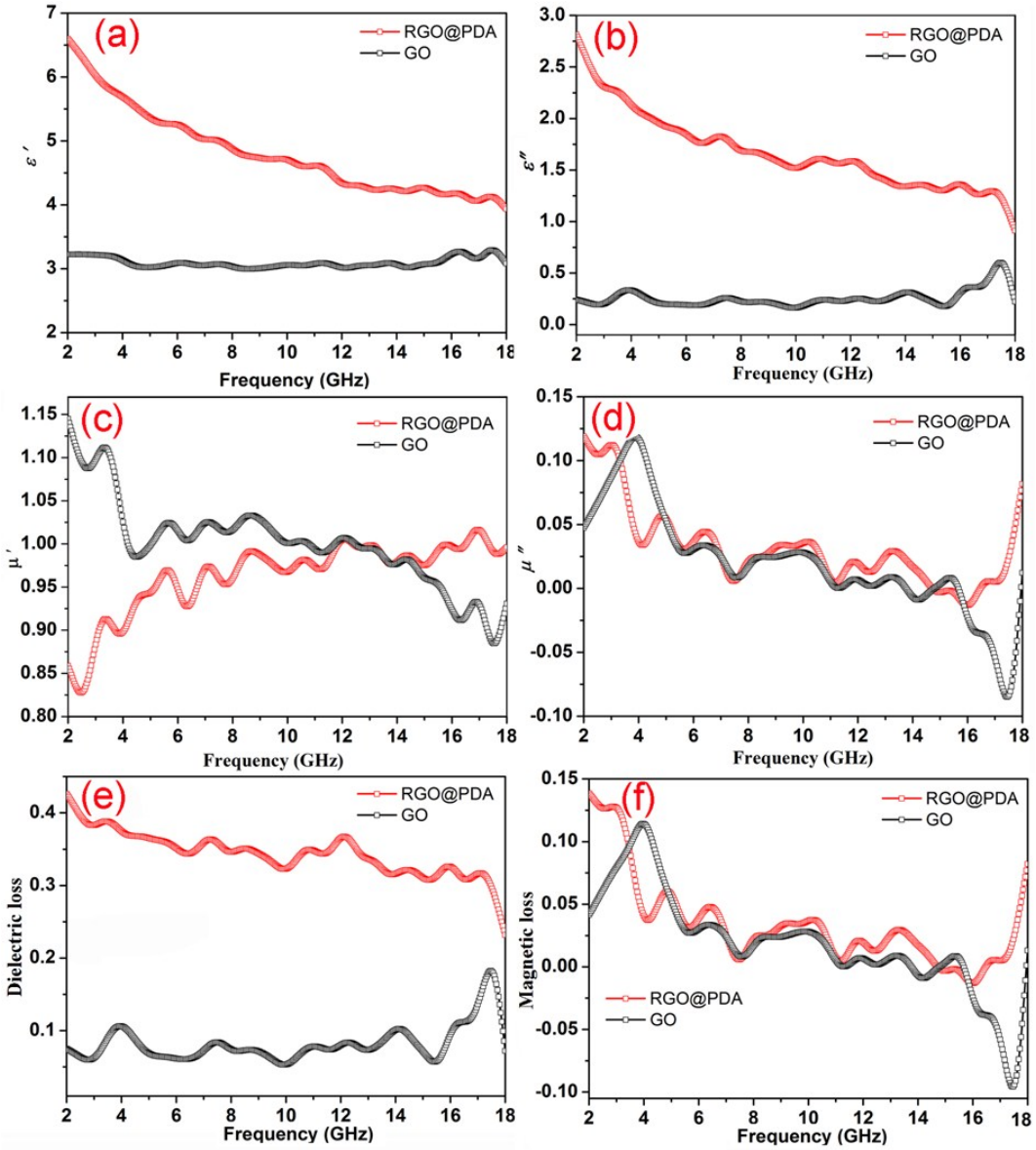

Fig. S3 Frequency dependence of the real part (a) and imaginary part (b) of complex permittivity and the real part (c) and imaginary part (d) of complex permeability, dielectric loss tangent (e) and magnetic loss tangent (f) for GO and RGO@PDA.

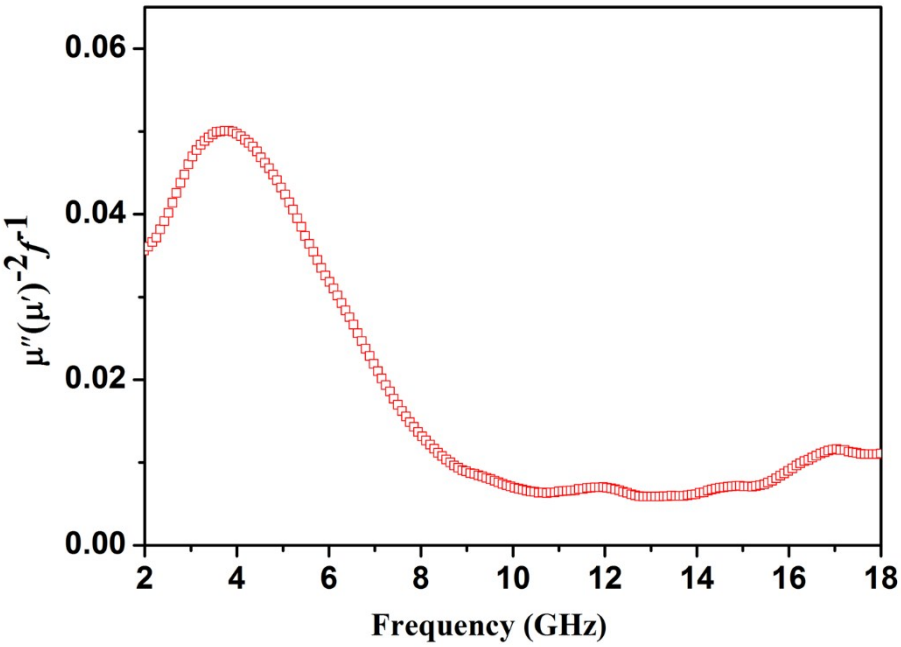

Fig. S4 Frequency dependence of $\mu''(\mu')^{-2}f^{1}$ for graphene@carbon@Fe_3O_4 nanosheet arrays.